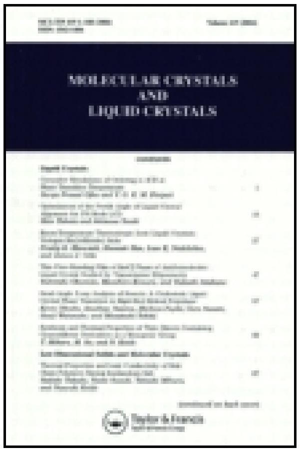

Molecular Crystals and Liquid Crystals Science and Technology. Section A. Molecular Crystals and Liquid Crystals

Publication details, including instructions for authors and subscription information:
http://www.tandfonline.com/loi/gmcl19

Syntheses and Physical Properties of Ferrocene Derivatives (VI) Crystal Structure of a Liquid Crystalline Ferrocene Derivative, [4-[6-(cholesteryloxycarbonyl) hexyloxycarbonyl]phenyl]ferrocene

Naotake Nakamura [a] & Taiki Takayama [a]

[a] Department of Chemistry, Faculty of Science and Engineering, Ritsumeikan University, 1-1-1, Nojihigashi, Kusatsu, Shiga, 525-77, Japan

To cite this article: Naotake Nakamura & Taiki Takayama (1997): Syntheses and Physical Properties of Ferrocene Derivatives (VI) Crystal Structure of a Liquid Crystalline Ferrocene Derivative, [4-[6-(cholesteryloxycarbonyl) hexyloxycarbonyl]phenyl]ferrocene, Molecular Crystals and Liquid Crystals Science and Technology. Section A. Molecular Crystals and Liquid Crystals, 307:1, 145-154

To link to this article: http://dx.doi.org/10.1080/10587259708047093

Mol. Cryst. Liq. Cryst., 1997, Vol. 307, pp. 145–154
Reprints available directly from the publisher
Photocopying permitted by license only

Syntheses and Physical Properties of Ferrocene Derivatives (VI) Crystal Structure of a Liquid Crystalline Ferrocene Derivative, [4-[6-(cholesteryloxycarbonyl) hexyloxycarbonyl]phenyl]ferrocene

NAOTAKE NAKAMURA and TAIKI TAKAYAMA

Department of Chemistry, Faculty of Science and Engineering,
Ritsumeikan University, 1-1-1, Nojihigashi, Kusatsu, Shiga 525-77, Japan

(Received 21 February 1997; In final form 25 March 1997)

The structure of monosubstituted ferrocene derivative which has a flexible spacer between the ferrocene and the mesogenic group, [4-[6-(cholesteryloxycarbonyl)hexyloxycarbonyl]phenyl]-ferrocene was determined by the X-ray diffraction method. The two crystallographically unequivalent molecules *A* and *B* exist in the unit cell. The molecular geometry is almost extended and linear, and the two cyclopentadienyl rings exhibit an eclipsed conformation rather than a staggered one in both molecules. The *gauche* conformation at the ferrocenyl side end of the hexyl chain in molecule *B* can be lead to efficient packing, in which the tetracyclic cores overlap antiparallel as well as avoid close contact with ferrocene in molecule *A*. The molecules are arranged in layers which is layers which is a precursor to a smectic phase.

Keywords: Crystal structure; ferrocene; monosubstituted ferrocene derivative; cholesteryl derivative; metallomesogen; liquid crystal

INTRODUCTION

Liquid crystalline compounds containing transition metal have been of great interest in recent years, because of their potentially unique electric, magnetic and chromatic properties. Ferrocene, one of the metallocenes, shows remarkable thermal stability and aromaticity. Although many ferrocene derivatives which exhibit liquid crystallinity have been synthesized hitherto [1], there are few reports on X-ray studies. In particular, single crystal X-ray structure analysis of these compounds has been carried out on only three compounds, 1,1'-[2], 1,3-disubstituted [3], and monosubstituted ferrocene derivatives [4]. However, the mesogenic group for these compounds is directly introduced into the cyclopentadienyl ring (henceforth abbreviated to Cp-ring) of ferrocene, and they have a flexible alkyl or alkoxy chain as a terminal group.

The phase transition behavior of monosubstituted ferrocene derivatives containing the cholesteryl group as a mesogenic one, [4-[ω-(cholesteryloxycarbonyl)alkoxycarbonyl]phenyl]ferrocene (henceforth abbreviated to CAPF-*n*, $n = 1-11$, and 15, where *n* is the number of carbon atoms in the methylene chain as a flexible spacer) has been investigated in our laboratory. Some of them (CAPF-2, 4, 6, 8, 9, 10, 11, and 15) exhibited liquid crystallinity [5, 6] and the liquid crystalline phases were identified with the smectic C by the small-angle scattering X-ray diffraction [7] method.

In this study, the crystal and molecular structure of CAPF-6 was determined by single-crystal X-ray diffraction in order to discuss the mechanism of the transition to the mesophase. To the best of our knowledge, this is the first example about X-ray crystal structure analysis of liquid crystalline monosubstituted ferrocene derivatives containing the flexible spacer between the ferrocene and the mesogenic group.

EXPERIMENTAL

The single crystal of the title compound was obtained from a solution of benzene and methanol by a slow evaporation method (3 months). An orange crystal having approximate dimensions $0.4 \times 0.2 \times 0.05$ mm was mounted on a goniometer head. All measurements were made on a Rigaku AFC5R diffractometer with graphite monochromated Cu-Kα radiation ($\lambda = 1.54178$ Å).

Unit cell parameters were obtained by a least-squares refinement using the setting angles of 25 carefully centered reflections in the range $46.4 < 2\theta < 57.0°$. The data were collected at 296 ± 1 K using the ω-2θ scan technique to a maximum 2θ value of 120.4°.

Of 7524 collected reflections, 7021 were unique. The intensities of three representative reflections were measured after every 150 reflections. Over the course of data collection, the standards decreased by -11.6%. A linear correction factor was applied to the data to account for this phenomenon.

The data were corrected for Lorentz and polarization effects and for absorption (Ψ scans [8]; $T_{min} = 0.835$, $T_{max} = 0.998$). The correction for secondary extinction was applied (Zachariasen type 2 Gaussian isotropic; coefficient = 7.60747).

The structure was solved by direct methods (SHELXS86 [9]) and expanded using Fourier techniques. All non-hydrogen atoms were refined anisotropically, while hydrogen atoms were included as fixed riding atoms in geometrically calculated positions. The final refinement was made by full-matrix least-squares based on 3195 observed reflections ($I > 3.0\ \sigma(I)$). Convergence was reached with unweighted and weighted agreement factors of:

$$R = \Sigma(|Fo| - |Fc|)/\Sigma|Fo| = 0.061$$

$$R_w = (\Sigma w(|Fo| - |Fc|)^2/\Sigma w Fo^2 = 0.079$$

where the weighted scheme $w = 1/[\sigma^2(Fo) + 0.00076\,Fo^2]$.

Final data may be obtained from the Cambridge Crystallographic Data Center, 12 Union Road, Cambridge, CB2 1EZ, UK.

RESULTS AND DISCUSSION

Data regarding collection and refinement are summarized in Table I. All calculations were performed using the teXsan [10] crystallographic software

TABLE I Crystal Data of CAPF-6

Empirical formula	$C_{51}H_{70}O_4Fe$
Formula weight	802.96
Crystal size/mm	0.4 × 0.2 × 0.05
Radiation	CuKα($\lambda = 1.54178$ Å)
Crystal system	monoclinic
Space group	$P2_1$
Lattice parameter	
a/Å	13.093(5)
b/Å	8.977(5)
c/Å	38.532(4)
β/°	93.17(2)
Volume/Å^3	4522(2)
Z value	4
D_{calc}/gcm^{-3}	1.179
F(000)	1736.0
μ(CuKα)/mm^{-1}	2.995
R	0.061
R_w	0.079

package of Molecular Structure Corporation. Fractional atomic coordinates and equivalent isotropic temperature factors are given in Table II.

The molecular structure of CAPF-6 is shown in Figure 1. The two crystallographically unequivalent molecules *A* and *B* exist in the unit cell. The bond distances and angles are in agreement with those of usual values observed in the organic compounds within an experimental error. The molecular geometry is almsot extended and linear in both molecules.

The planes listed in Table III are defined as follows: Plane 1: substituted Cp-ring; Plane 2: unsubstituted Cp-ring; Plane 3: phenyl ring; Plane 4: C(17), O(1), O(2); Plane 5: tetracyclic cores of cholesteryl group. The two Cp-rings (Plane 1 and 2) run parallel to each other with dihedral angles of 3.9(6) and 1.9(1)° for molecules *A* and *B*, respectively. Also, the mean values of the five dihedral angles between least-squares planes (exocyclic C, Cg1, Fe, Cg2, exocyclic C; where Cg is a Cp-ring centroid, 1 and 2 are corresponding to the substituted Cp-ring and the unsubstituted Cp-ring, respectively) are 6.2(9)° for molecule *A* and 6.0(1)° for molecule *B*. Therefore, the two Cp-rings in both molecules have an eclipsed conformation rather than a staggered one which has been observed for disubstituted ferrocene derivatives [2, 3]. The eclipsed conformation of this kind has been observed in other monosubstituted ferrocene derivatives [12, 13]. The substituted Cp-ring (Plane 1), the adjacent phenyl ring (Plane 3) and the neighboring ester linkage (Plane 4) for both molecules are nearly coplanar. The tetracyclic cores (Plane 5) are out of the plane of the substituted Cp-ring (Plane 1), as indicated by dihedral angles of 122.5(6) and 27.6(3)° for molecules *A* and *B*, respectively.

The intramolecular distance C(26)...C(40), which is useful for comparing the length of the tetracyclic core, is estimated 8.9(2) Å long in molecule *A* 8.9(8) Å long in molecule *B*. These parameters are nearly equal to those of other related molecules (8.86–9.01 Å) [12–14]. The conformation of the tetracyclic cores can be validated as an slightly twist, of which the torsion angles C(49)-C(36)-C(28)-C(48) are 6.1° in molecule *A* and 5.2° in molecule *B*. These angles are between 7.9° and 12.0° in a series of cholesteryl *n*-alkanoates [12–14].

The ferrocenylphenylester groups and the tetracyclic cores in both molecules have very similar conformations, but a few discrepancies are observed in part of the ester functions connecting with the cholesteryl group, in the C(41) substituents, and in the hexyl chains as the flexible spacer. Selected torsion angles are given in Table IV.

The torsion angles C(24)-O(3)-C(25)-C(30) is − 105(1)° in molecule *A* and − 150(1)° in molecule *B*. One of the major differences in molecules *A* and *B*

TABLE II Fractional atomic coordinates and equivalent isotropic temperature factors

	x	y	z	B_{eq}
Molecule A				
Fe(1)	0.3380(2)	0.3825	0.20986(6)	6.35(7)
O(1)	0.417(1)	0.019(2)	0.0432(3)	9.1(4)
O(2)	0.560(1)	0.154(2)	0.425(3)	10.5(5)
O(3)	0.3658(10)	0.335(1)	−2.003(3)	8.2(4)
O(4)	0.343(1)	0.095(2)	−1.870(3)	10.6(5)
C(1)	0.428(1)	0.226(2)	0.2013(4)	6.6(5)
C(2)	0.483(1)	0.340(2)	0.2213(4)	6.2(4)
C(3)	0.429(1)	0.361(2)	0.2526(3)	7.2(5)
C(4)	0.345(1)	0.256(2)	0.2508(4)	7.5(5)
C(5)	0.344(1)	0.188(2)	0.2187(4)	6.6(5)
C(6)	0.304(2)	0.488(5)	0.1604(6)	13(1)
C(7)	0.343(2)	0.594(3)	0.1833(7)	10.0(8)
C(8)	0.277(2)	0.611(3)	0.2125(6)	10.7(8)
C(9)	0.200(1)	0.510(4)	0.2071(9)	12.2(9)
C(10)	0.217(2)	0.433(3)	0.1764(7)	11.2(9)
C(11)	0.452(1)	0.183(2)	0.1665(4)	6.4(5)
C(12)	0.531(1)	0.245(2)	0.1483(4)	8.1(5)
C(13)	0.541(2)	0.214(2)	0.1133(5)	8.9(6)
C(14)	0.474(1)	0.121(2)	0.0954(4)	6.9(5)
C(15)	0.402(1)	0.047(2)	0.1134(5)	8.4(6)
C(16)	0.392(1)	0.076(2)	0.1478(4)	8.2(6)
C(17)	0.492(2)	0.099(3)	0.0581(5)	8.7(7)
C(18)	0.425(2)	−0.008(3)	0.0068(5)	10.9(7)
C(19)	0.378(2)	0.115(3)	−0.0140(4)	10.2(7)
C(20)	0.381(2)	0.072(3)	−0.0537(5)	12.0(8)
C(21)	0.363(1)	0.202(3)	−0.0783(4)	9.2(6)
C(22)	0.364(2)	0.155(3)	−0.1156(4)	10.1(6)
C(23)	0.354(1)	0.277(3)	−0.1420(4)	9.2(6)
C(24)	0.354(2)	0.227(2)	−0.1799(4)	5.7(5)
C(25)	0.362(1)	0.302(2)	−0.2377(3)	7.4(5)
C(26)	0.294(1)	0.419(2)	−0.2544(4)	6.7(5)
C(27)	0.294(2)	0.406(2)	−0.2936(3)	5.0(4)
C(28)	0.3971(10)	0.401(2)	−0.3099(3)	5.3(4)
C(29)	0.467(1)	0.285(2)	−0.2892(3)	5.5(4)
C(30)	0.471(1)	0.310(2)	−0.2494(4)	7.8(5)
C(31)	0.206(1)	0.400(2)	−0.3119(4)	5.4(4)
C(32)	0.1946(9)	0.391(2)	−0.3503(3)	5.3(4)
C(33)	0.2928(9)	0.431(1)	−0.3676(3)	4.1(3)
C(34)	0.3831(9)	0.345(2)	−0.3486(3)	5.3(4)
C(35)	0.2852(9)	0.378(2)	−0.4050(3)	4.4(3)
C(36)	0.3828(8)	0.403(2)	−0.4256(3)	4.1(3)
C(37)	0.4664(10)	0.311(2)	−0.4067(3)	5.8(4)
C(38)	0.4809(9)	0.352(2)	−0.3681(3)	5.3(4)
C(39)	0.2001(10)	0.449(2)	−0.4296(3)	5.4(4)
C(40)	0.2316(9)	0.412(2)	−0.4659(3)	5.8(4)
C(41)	0.3424(9)	0.351(2)	−0.4621(3)	4.3(3)
C(42)	0.4037(10)	0.393(2)	−0.4936(3)	5.6(4)
C(43)	0.350(1)	0.336(2)	−0.5276(3)	6.3(4)
C(44)	0.3821(10)	0.403(2)	−0.5606(3)	6.5(4)
C(45)	0.318(1)	0.353(3)	−0.5931(4)	8.9(6)

TABLE II (Continued)

C(46)	0.345(1)	0.434(3)	−0.6270(4)	10.1(7)
C(47)	0.269(2)	0.397(5)	−0.6557(4)	16(1)
C(48)	0.444(1)	0.556(2)	−0.3063(3)	5.9(4)
C(49)	0.4149(10)	0.568(2)	−0.4267(4)	5.7(4)
C(50)	0.514(1)	0.344(2)	−0.4912(4)	8.3(6)
C(51)	0.442(1)	0.393(4)	−0.6375(5)	13.5(9)
Molecule B				
Fe(1′)	0.1530(2)	0.6524(5)	0.03998(7)	8.77(9)
O(1′)	0.1069(8)	0.866(1)	0.2315(2)	7.2(3)
O(2′)	−0.0433(9)	0.748(2)	0.2279(3)	8.6(4)
O(3′)	0.0931(6)	0.894(1)	0.4686(2)	5.8(2)
O(4′)	0.2321(10)	0.773(2)	0.4532(3)	9.5(4)
C(1′)	0.057(2)	0.810(3)	0.0671(4)	9.4(7)
C(2′)	−0.001(1)	0.715(3)	0.0423(6)	10.1(7)
C(3′)	0.034(2)	0.748(4)	0.0080(5)	12(1)
C(4′)	0.112(2)	0.851(3)	0.0102(5)	10.6(8)
C(5′)	0.119(2)	0.896(3)	0.0482(5)	11.3(8)
C(6′)	0.236(3)	0.557(6)	0.0767(5)	17(1)
C(7′)	0.176(3)	0.464(4)	0.053(1)	15(1)
C(8′)	0.199(2)	0.475(4)	0.0230(10)	13(1)
C(9′)	0.274(2)	0.574(4)	0.0211(5)	12.6(9)
C(10′)	0.301(2)	0.634(4)	0.0534(8)	13.2(10)
C(11′)	0.050(1)	0.816(2)	0.1043(4)	7.2(5)
C(12′)	−0.029(1)	0.742(3)	0.1184(4)	8.4(6)
C(13′)	−0.040(1)	0.742(2)	0.1543(5)	7.7(5)
C(14′)	0.035(1)	0.812(2)	0.1758(4)	6.5(5)
C(15′)	0.111(1)	0.884(3)	0.1604(4)	8.5(6)
C(16′)	0.122(1)	0.891(3)	0.1258(4)	9.6(6)
C(17′)	0.026(2)	0.812(2)	0.2132(4)	7.2(5)
C(18′)	0.110(1)	0.844(2)	0.2687(3)	8.7(6)
C(19′)	0.201(1)	0.925(2)	0.2834(4)	7.8(5)
C(20′)	0.234(1)	0.874(3)	0.3209(5)	10.4(6)
C(21′)	0.163(1)	0.911(2)	0.3463(4)	8.1(5)
C(22′)	0.200(1)	0.867(3)	0.3846(3)	8.4(5)
C(23′)	0.131(1)	0.909(2)	0.4105(3)	6.7(4)
C(24′)	0.161(1)	0.851(2)	0.4463(3)	5.6(4)
C(25′)	0.109(1)	0.846(2)	0.5042(3)	5.7(4)
C(26′)	0.177(1)	0.959(2)	0.5244(3)	5.6(4)
C(27′)	0.1805(10)	0.932(1)	0.5623(3)	4.3(3)
C(28′)	0.0807(9)	0.907(2)	0.5799(3)	4.3(3)
C(29′)	0.014(1)	0.799(2)	0.5571(3)	6.1(4)
C(30′)	0.005(1)	0.836(2)	0.5182(3)	6.4(4)
C(31′)	0.2703(10)	0.932(2)	0.5812(3)	4.4(3)
C(32′)	0.2842(9)	0.912(2)	0.6189(3)	4.7(3)
C(33′)	0.1835(9)	0.928(2)	0.6379(3)	4.1(3)
C(34′)	0.0978(9)	0.841(2)	0.6166(3)	4.3(3)
C(35′)	0.1970(10)	0.862(2)	0.6744(3)	4.5(3)
C(36′)	0.0974(9)	0.868(2)	0.6945(3)	4.6(4)
C(37′)	0.0216(9)	0.768(2)	0.6734(3)	4.9(4)
C(38′)	0.0017(9)	0.825(2)	0.6367(3)	5.3(4)
C(39′)	0.278(1)	0.932(2)	0.6995(3)	5.6(4)
C(40′)	0.249(1)	0.872(2)	0.7350(3)	6.2(4)
C(41′)	0.1435(10)	0.799(2)	0.7293(3)	4.9(4)
C(42′)	0.083(1)	0.813(2)	0.7625(3)	5.9(4)

TABLE II (Continued)

C(43′)	0.143(1)	0.740(2)	0.7939(4)	7.0(5)
C(44′)	0.097(1)	0.766(2)	0.8284(3)	8.3(5)
C(45′)	0.156(1)	0.689(3)	0.8576(4)	8.5(5)
C(46′)	0.123(2)	0.708(4)	0.8924(5)	14(1)
C(47′)	0.175(2)	0.604(3)	0.9195(4)	10.8(7)
C(48′)	0.025(1)	1.063(2)	0.5800(4)	6.4(4)
C(49′)	0.056(1)	1.023(2)	0.6998(4)	6.6(5)
C(50′)	−0.021(1)	0.739(3)	0.7563(3)	8.7(6)
C(51′)	0.061(3)	0.808(5)	0.9022(6)	23(1)

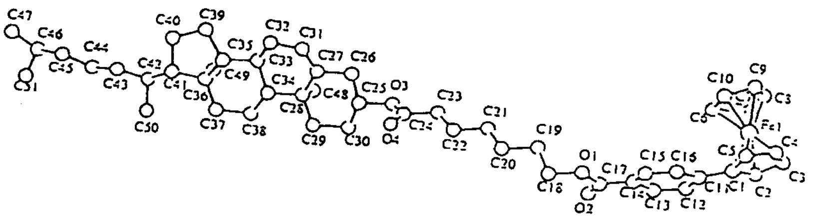

Molecule A

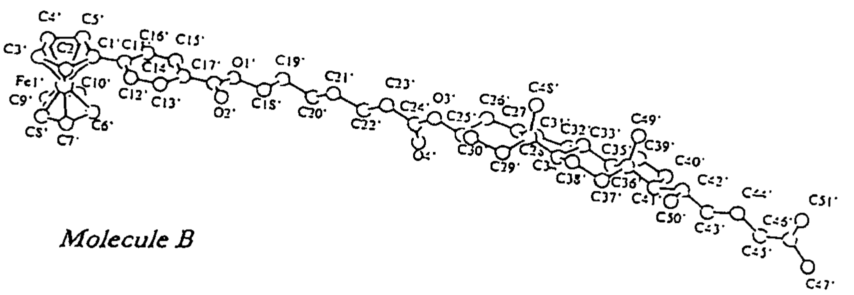

Molecule B

FIGURE 1 ORTEP view [11] of the two unequivalent molecules, showing the crystallographic numbering scheme.

is caused by the difference of −45° in the rotation at the cholesteryl-side ester bond. The terminal side chain from C(41) in molecules *A* and *B* is almost fully extended, although the last three atoms, C(46), C(47), and C(51) are ill-defined because of somewhat large thermal motions. The most interesting feature of the two independent molecules is the conformation with respect to the flexible hexyl chain. In the sequence of bonds from C(19)-C(20) through to C(22)-C(23), the torsion angles are 164(2), −179(1), −176(1),

TABLE III Dihedral angles between least-squares planes for CAPF-6

Plane 1: substituted Cp-ring
Plane 2: unsubstituted Cp-ring
Plane 3: phenyl ring
Plane 4: C(17), O(1), O(2)
Plane 5: tetracyclic core of cholesteryl group

Plane	*Angle/°*	
	Molecule A	*Molecule B*
Plane 1–Plane 2	3.96	1.91
Plane 1–Plane 3	12.21	12.47
Plane 3–Plane 4	171.15	170.33
Plane 1–Plane 5	122.56	27.63
Plane 3–Plane 5	123.66	15.19
Plane 4–Plane 5	48.67	170.82

TABLE IV Selected torsion angles for CAPF-6

atom atom atom atom	*Angle/°*	
	Molecule A	*Molecule B*
C(18)—C(19)—C(20)—C(21)	− 164(2)	− 66(2)
C(19)—C(20)—C(21)—C(22)	− 179(1)	− 176(1)
C(20)—C(21)—C(22)—C(23)	− 176(1)	177(1)
C(21)—C(22)—C(23)—C(24)	− 179(1)	172(1)
C(24)—O(3)—C(25)—C(30)	− 105(1)	− 150(1)
C(36)—C(41)—C(42)—C(50)	56(1)	59(1)
C(36)—C(41)—C(42)—C(43)	− 177(1)	− 178(1)
C(41)—C(42)—C(43)—C(44)	163(1)	172(1)
C(42)—C(43)—C(44)—C(45)	− 174(1)	177(1)
C(43)—C(44)—C(45)—C(46)	174(1)	177(2)
C(44)—C(45)—C(46)—C(47)	− 171(2)	169(2)
C(44)—C(45)—C(46)—C(51)	68(2)	− 15(5)

and − 179(1)° in molecule *A*. However, there is no such regularity in molecule *B*, where the corresponding angles are − 66(2), − 176(1), − 177(1), and 172(1)°. Consequently, the overall molecular shape for molecule *B*, which has one *gauche* conformation, becomes more linear than that of molecule *A*.

The molecules are packed in an antiparallel fashion overlapping the tetracyclic cores, as observed in cholesteryl *n*-alkanoates [12–14], and are oriented along the *c*-axis, as presented in Figure 2. The individual molecule is arranged in a head-to-tail manner and there is deep penetration up to about 10 Å of ferrocenylphenylester group in molecule *A* from the neighboring unit. The *gauche* conformation at the ferrocenyl side end of the hexyl chain in molecule *B* could be lead to very efficient packing, in which the tetracyclic

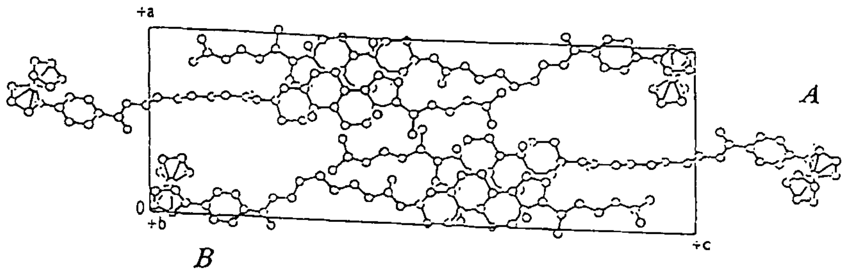

FIGURE 2 Packing diagram viewed along the *b*-axis.

cores overlap with an antiparallel array and also the hexyl chain in molecule *B* avoids close contact with ferrocene in molecule *A*. The lengths of the long molecular axis are 34.9 Å for molecule *A* and 34.7 Å for molecule *B*. These values coincide with the calculated model molecular length (34.4 Å). However, the molecules are arranged to form layers which have a length of about 48 Å between the ferrocene moieties in molecules *A* and *B*. The direction of this length is approximately parallel to the [−3 0 1] crystal axis, which makes an angle of about 80° with respect to the layer interface of the *a*-axis, and the layer interval is about 47.5 Å long.

The phase transition behavior of CAPF-6 was observed [5] as follows: the melting behavior of the as-grown sample was observed at 332 K on the 1st heating. On the 1st cooling, the molten sample changed into the mesophase at 324 K, and went into the glass state at 300 K. On the 2nd heating, the transformations were glass state to mesophase (300 K), and to isotropic liquid (325 K), successively.

The layer spacing of CAPF-6 in the mesophase was estimated to be about 65 Å long by two different kinds of small-angle scattering X-ray diffraction measurements equipped with two different kinds of detector [6, 7]. It has been proposed previously that the mesophase could be identified with the smectic C phase, which has two molecules in the layers and has a tilt angle of about 60°, because of the comparison of the layer spacing with the calculated model molecular length [6, 7].

Therefore, in regard to the transition to the mesophase, it is inferred that molecules *A* and *B* will not only slide along the molecular long axis, opposite to each other, but also the tilt angle of the molecules change from about 80° in the crystalline phase to about 60° to the layer interface because of freedom in the flexible hexyl chains. As a result, the molecules may be arranged in antiparallel fashion without overlapping the tetracyclic cores. In the proposed structure of the mesophase, the layer spacing is estimated to be about 61 Å long. This value is comparable to that of experimental value (65 Å) in which layer–layer interval spacing included [7]. Consequently, the mesophase could be regarded as the smectic C phase, which is in accordance with the result obtained from small-angle scattering X-ray diffraction experiments already reported [7].

Acknowledgements

This study was partially supported by the Ritsumeikan University Foundation Memorial Trust Research Fund and The Science Research Promotion Fund of Japan Private School Promotion Foundation.

References

[1] J. Malthete and J. Billard, *Mol. Cryst. Liq. Cryst., Lett.*, **34**, 117 (1976).
[2] M. A. Khan, J. C. Bhatt, B. M. Fung and K. M. Nicholas, *Liquid Crystals*, **5**, 285 (1989).
[3] R. Deschnaux, I. Kozstics, J.-L. Marendaz and H. Stoeckli-Evans, *Chimia*, **47**, 206 (1993).
[4] C. Loubser, C. Imrie and P. H. van Rooyen, *Adv. Mater.*, **5**, 45 (1993).
[5] N. Nakamura, T. Hanasaki and H. Onoi, *Mol. Cryst. Liq. Cryst.*, **225**, 269 (1993).
[6] N. Nakamura, T. Hanasaki, H. Onoi and T. Oida, *Chem. Express*, **8**, 467 (1993).
[7] N. Nakamura, T. Oida, M. Shonago, H. Onoi and T. Hanasaki, *Mol. Cryst. Liq. Cryst.*, **265**, 1 (1995).
[8] A. C. T. North, D. C. Phillips and F. S. Mathews, *Acta. Cryst.*, **A24**, 351 (1968).
[9] G. M. Sheldrick, *SHELXS86. Crystallographic Computing* **3**, edited by G. M. Sheldrick, C. Krüger and R. Goddard, Oxford University Press, London, pp. 175–189 (1985).
[10] Molecular Structure Corporation. *teXsan.* Single Crystal Structure Analysis Software. Version 1.7. MSC, 3200 Research Forest Drive, The Woodlands, TX 77381, USA (1995).
[11] C. K. Johnson, *ORTEPII*, A FORTRAN Thermal-Ellipsoid Plot Program, Report ORNL-5138, Oak Ridge National Laboratory, Oak Ridge, Tennessee, USA (1976).
[12] R. M. G. Roberts, J. Silver, B. M. Yamin, M. G. B. Drew and U. Eberhardt, *J. Chem. Soc., Dalton Trans.*, 1549 (1988).
[13] G. Ferguson, J. F. Gallagher, C. Glidewall and C. M. Zakaria, *Acta Cryst.*, **C49**, 967 (1993).
[14] B. M. Craven and G. T. DeTitta, *J. Chem. Soc. Perkin II.*, 814 (1976).
[15] N. G. Guerina and B. M. Craven, *J. Chem. Soc. Perkin II.*, 1414 (1979).
[16] V. Pattabhi and B. M. Craven *J. Lipid Res.*, **20**, 753 (1979).